

Organic--Inorganic Layer Compounds: Physical Properties and Chemical Reactions

P. Day

Phil. Trans. R. Soc. Lond. A 1985 **314**, 145-158

doi: 10.1098/rsta.1985.0015

Email alerting service

Receive free email alerts when new articles cite this article - sign up in the box at the top right-hand corner of the article or click [here](#)

To subscribe to *Phil. Trans. R. Soc. Lond. A* go to: <http://rsta.royalsocietypublishing.org/subscriptions>

Organic–inorganic layer compounds: physical properties and chemical reactions

BY P. DAY

Oxford University Inorganic Chemistry Laboratory, South Parks Road, Oxford OX1 3QR, U.K.

In contrast with intercalation compounds, which can exist both with and without organic molecules between the planes of inorganic material, ‘molecular composite’ compounds have organic groups covalently or ionically bound to inorganic layers. In such crystals the aim is to combine magnetic or optical properties characteristic of the inorganic solid state, like magnetism and luminescence, with properties found in the organic solid state like mesomorphism or polymerization. This contribution surveys experiments from our laboratory on the structural, physical and chemical properties of one series of ‘molecular composites’, the layer perovskite halide salts $(\text{RNH}_3)_2\text{MX}_4$ (R = organic group; M = Cr, Mn, Cd; X = Cl, Br). When R is an *n*-alkyl group these compounds undergo structural phase transitions triggered by variations in the hydrogen-bonding of the $-\text{NH}_3$ to the inorganic layer. Optical microscopy is used to follow the phase transitions and map ferroelastic domains. Compounds with M = Cr are ferromagnets with strongly temperature-dependent visible absorption spectra, whose intensity correlates with the degree of magnetic order. In Mn and Cd salts more elaborate functional groups can be inserted in the organic sidechains with the aim of making topochemical polymerizations in the solid state.

1. INTRODUCTION: MOLECULAR COMPOSITES

The purpose of this paper is to introduce some of the unusual physical and chemical properties that can arise when organic groups are interleaved between layers of inorganic ions or molecules by covalent or ionic bonding to form a ‘molecular composite’ (Day & Ledsham 1982). By this term we wish to distinguish such compounds from the more familiar intercalated layer systems like graphite or TaS_2 , which can exist independently of guest molecules placed between their layers. Further, the stoichiometric ratio of host to guest in a conventional intercalate may vary, while in a ‘molecular composite’ the proportion of organic to inorganic material is fixed by the requirements of covalent or ionic bonding. Because the organic molecules are directly bonded to the inorganic layer, not only their stoichiometry but their orientation is fixed, in contrast to intercalated molecules, which may be translationally mobile. As a result such compounds can often be obtained as fully ordered single crystals.

In view of the stereospecific alignment of organic molecules between the inorganic layers in ‘molecular composites’ an attractive possibility is to use them as matrices for solid state polymerization of ordered monomers according to the topochemical principle. Experiments of this kind are described in §5, but I also wish to draw attention in this introduction to the opportunity presented by molecular composites for fabricating crystalline structures combining the physical properties characteristic of organic molecular and inorganic lattice structures on a molecular scale. Some of the properties in question are indicated schematically in figure 1. For example, one might envisage a layer or chain of localized magnetic moments, as on

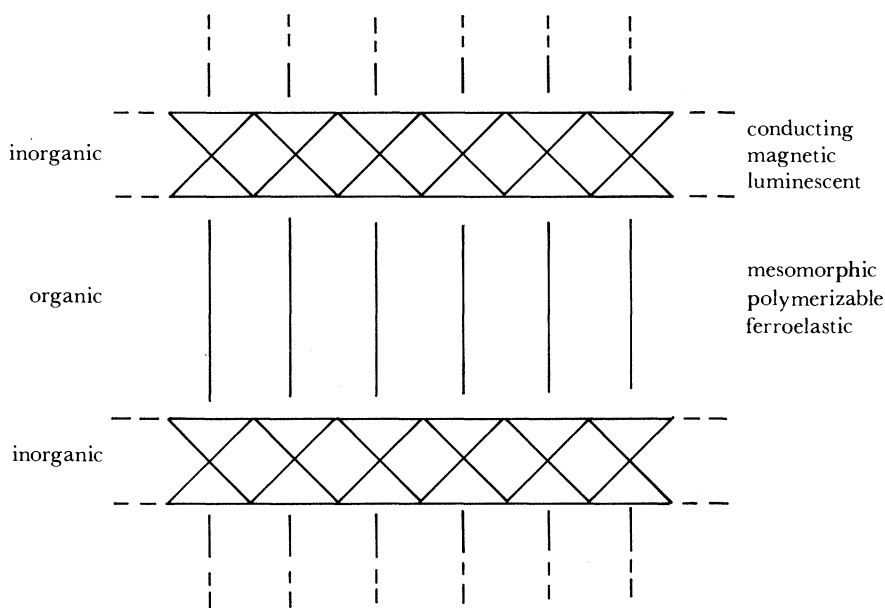


FIGURE 1. Some possible properties in organic-inorganic molecular composite crystals.

transition metal ions, whose order might be triggered by a small variation in superexchange pathway induced by a structural phase transition on rotating attached organic sidechains. Another possibility, not yet achieved synthetically, is a chain of mixed valency metal ions coordinated to conjugated groups in such a way that electrons transported along the chain could couple with electrons in the polarizable side-groups. This was an early recipe (still not realized!) for an excitonic superconductor (Little 1964).

Chemical bonding between the organic groups and the inorganic layers may be covalent, ionic or by electron donation from a ligand to a metal ion, as in a coordination complex. An example of covalently linked groups is the phosphoric ester addition compounds of $\text{Zr}(\text{HPO}_4)_2\text{H}_2\text{O}$. Reaction of the parent compound with $\text{RO}(\text{PO}_3)$, $\text{R} = n\text{-alkyl}$, gives $\text{Zr}(\text{HPO}_4)(\text{RPO}_4)_y\text{H}_2\text{O}$ with alkyl chains up to $\text{C}_{18}\text{H}_{37}$, in which the extended alkyl chains are packed at an angle of 34° to the Zr phosphate layer (Yamanaka *et al.* 1981). Coordination attachment occurs between long chain aliphatic n -alkylamines and Ni^{II} in layer compounds with cyanide bridges between adjacent Ni^{II} (Mathey *et al.* 1980). However, the composites available in greatest variety up till now are the layer perovskite halide salts.

2. LAYER PEROVSKITE HALIDE SALTS

This widespread group of salts has the general formula $(\text{RNH}_3)_2\text{MX}_4$, where M is a divalent cation, X a halide ion and R one of a wide range of organic moieties (Arend *et al.* 1978). Their structures closely resemble the K_2NiF_4 structure, which consists of layers of NiF_6 octahedra linked into a square array by sharing equatorial vertices. The layers are infinite anions of stoichiometry $(\text{MX}_4)_n^{2n-}$ and in the layer perovskite halide salts the $-\text{NH}_3^+$ ends of the cations occupy almost the same sites as K^+ in K_2NiF_4 . Chains attached to $-\text{NH}_3^+$ extend away from the inorganic layer on either side, as shown in figure 2. A spatial constraint on the R groups that can be incorporated is set by the 'area' of the $(\text{MX}_4)_n^{2n-}$ layer that each RNH_3^+ may cover, while maintaining Van der Waals contact with one another. Within that constraint, a wide

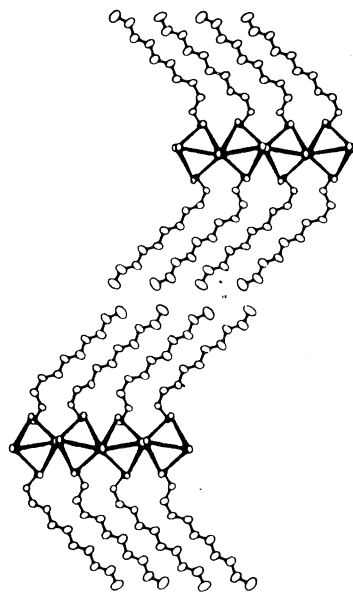


FIGURE 2. The crystal structure of $(C_{10}H_{21}NH_3)_2CdCl_4$ (Kind *et al.* 1979).

variety is possible, as exemplified in §5, though the main emphasis has been on extended alkyl chains.

The layer perovskite halide salts merit attention from three separate points of view. Because they can be prepared with different 3d-block elements (Cr, Mn, Fe, Cu), and the layers separated in a controllable way by varying the length of the alkyl sidechains, they are excellent models for two-dimensional cooperative magnetism. The Cr salts (referred to in more detail in §4) and Cu salts have near-neighbour ferromagnetic exchange while the Mn (Van Amstel & de Jongh 1971) and Fe (Mostafa & Willett 1971) examples are antiferromagnetic. Because the $-NH_3^+$ groups are attached to the $(MX_4)_n^{2n-}$ layers by weak hydrogen-bonding to the axial and equatorial X, many layer perovskite halide salts, including those containing non-magnetic (Cd) as well as magnetic ions, undergo complicated series of structural phase transitions (Blinic *et al.* 1977). These are driven by changes in the permutations of N-H---X combinations and lead at high temperatures to free rotation of $-NH_3^+$ and 'melting' of the long organic chains. Indeed, analogies have been drawn between such crystalline phase transitions and those of lipid bilayers (Kind *et al.* 1979). The third area of interest in layer perovskite halides is the possibility of using the inorganic layers as templates to hold organic moieties in regular arrays so that they could be induced to react with each other stereospecifically to form ordered polymers by means of the topochemical principle (Ledsham & Day 1981). This paper will review briefly work in our laboratory on all three aspects of the physics and chemistry of this class of molecular composites.

3. STRUCTURAL PHASE TRANSITIONS: TWINNING DOMAINS

There is an inherent dissymmetry in the layer perovskite salts $(RNH_3)_2MX_4$ between the threefold symmetry of the $-NH_3^+$ and the fourfold symmetry of the $(MX_4)_n^{2n-}$ layer. One result of this is that unless the $-NH_3^+$ is freely rotating (which is the case in the high-temperature tetragonal, h.t.t., phase) it cannot make equivalent contacts with the X atoms. The succession

of phases found arises from changes in the number of H bonded to equatorial bridging X within the basal plane or axial X above and below the plane. So, for example, $(\text{CH}_3\text{NH}_3)_2\text{MnCl}_4$ undergoes a second-order transition at 394 K from the h.t.t. phase (space group I4/mmm) to a room-temperature orthorhombic phase (r.t.o., Cmca) stable down to room temperature, in which each $-\text{NH}_3^+$ has one H hydrogen-bonded to an axial Cl and two to equatorial Cl (Arend & Granicher 1976). Below room temperature are further transitions, first to another tetragonal phase (l.t.t.) and finally to a monoclinic one. The l.t.t. phase has a superlattice based on an alternation of $-\text{NH}_3^+$ with one H bonded to an equatorial Cl and two to axial Cl with others having one H bonded axially and two equatorially (Heger *et al.* 1976).

The structures of these phases have been determined by X-ray and neutron diffraction and the mechanisms of the transitions by vibrational spectroscopy, inelastic neutron scattering, birefringence (Heygstar & Kleeman 1977) and thermal analysis. Less extensively studied, however, is one of the most easily observed features of the crystals, their crystallographic twinning domains. Depending on the method of preparation, and history, all crystals of layer perovskite salts with shorter alkyl sidechains show very pronounced twinning in the r.t.o. phase, the twinning plane being (110) so that the extinction directions under crossed polarizers lie at 45° to the twin boundaries (Arend *et al.* 1973). Examples are shown in figure 3. The morphology of these domains can be followed conveniently by temperature-programmed hot-stage microscopy. Of particular interest is the manner in which the domain walls are re-formed, and propagate through the crystal after its temperature has been raised through the r.t.o. to h.t.t. transition or lowered through the r.t.o. to l.t.t. transition, held in either tetragonal phase for varying lengths of time, and then brought back into the r.t.o. phase at different rates (Avery 1984).

The three micrographs in figure 3 illustrate the effect on a crystal of $(\text{CH}_3\text{NH}_3)_2\text{MnCl}_4$ of annealing at 126°C (5°C above the r.t.o.–h.t.t. transition temperature) for increasing lengths of time and then reducing the temperature to reform the r.t.o. phase. It can be seen that the crystal retains a clear ‘memory’ of the previous domain wall positions, only partly lost after the longest annealing period, when additional domains have been introduced. One must conclude that the twins nucleate at defects or dislocations at the edges of the crystal and then propagate across it. Evidence for this hypothesis comes from the observation of partly formed twins (see as thin wedges, marked w), which probably originate from a small lateral temperature gradient.

After a number of temperature cycles, or under the influence of stress, the density of twins increase to the point where the boundaries of adjacent twins interact. The tendency is then for the walls to become equally spaced. In proportion that this becomes the case the crystal can be made to function as a diffraction grating since light is scattered from the domain boundaries. Figure 4 shows a diffraction pattern obtained by passing light from a He–Ne laser (632.8 nm) through a crystal of $(\text{CH}_3\text{NH}_3)_2\text{MnCl}_4$. From the separation of the diffraction peaks a mean domain spacing of $11\ \mu\text{m}$ is estimated. More precise information on the distribution of domain widths could be obtained by Fourier transformation of the diffracted intensity. The diffraction vanishes as the crystal passes into the h.t.t. phase, so one might consider a temperature-dependent optical deflector.

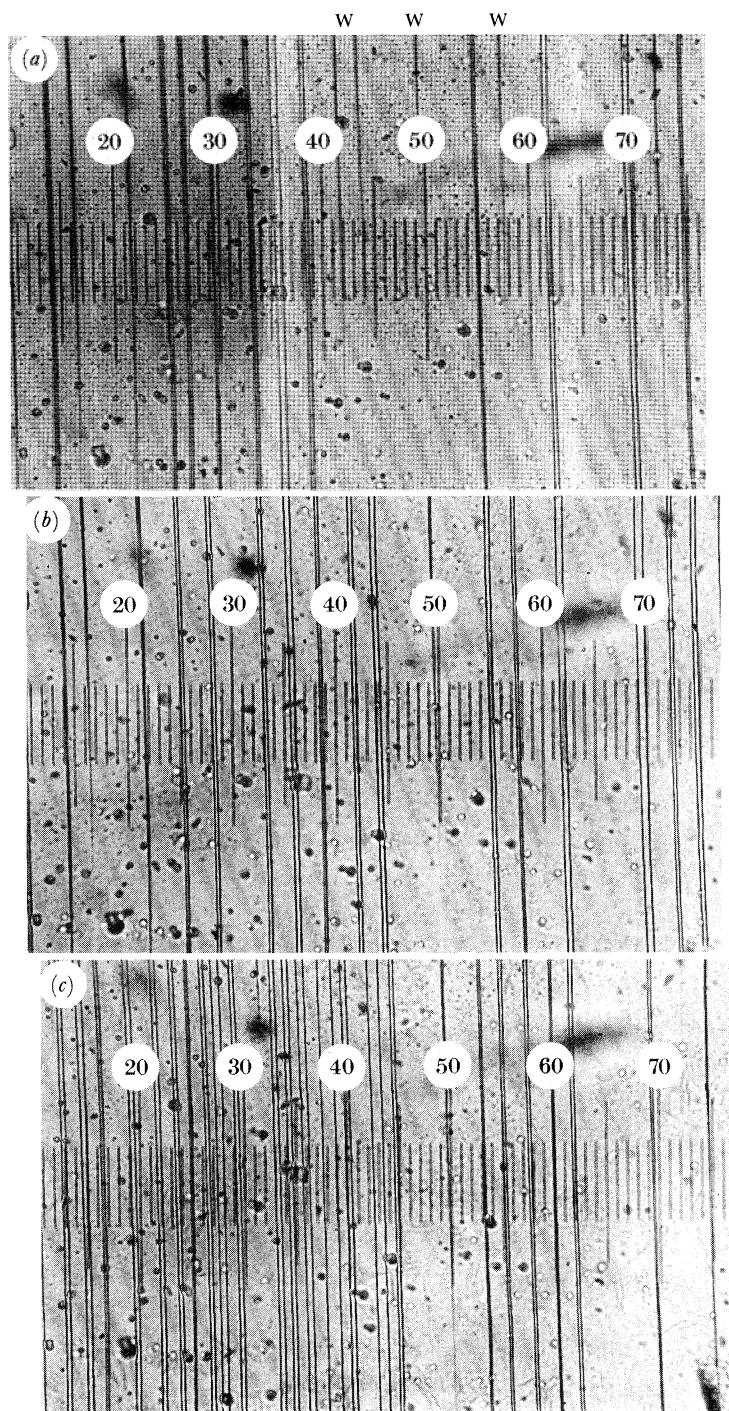


FIGURE 3. Twinning domains in a crystal of $(\text{CH}_3\text{NH}_3)_3\text{MnCl}_4$ after heating through the r.t.o. \rightarrow h.t.t. phase transition, annealing for different times and cooling. Annealing times are (a) 10 min (b) 100 min (c) 900 min.



FIGURE 4. Optical diffraction pattern from transmission of 6328 Å light through a crystal of $(\text{CH}_3\text{NH}_3)_2\text{MnCl}_4$ at room temperature.

4. TWO-DIMENSIONAL FERROMAGNETISM: LIGAND-FIELD SPECTRA AND MAGNETIC ORDER

Only a few ionic transition metal compounds with localized magnetic moments exhibit ferromagnetic near-neighbour exchange. Thus the layer perovskite halide salts $(\text{RNH}_3)_2\text{CuX}_4$ ($\text{X} = \text{Cl}, \text{Br}$) have been the subject of many studies as prototypes of two-dimensional ferromagnetism (de Jongh & Miedema 1974). The ferromagnetic exchange in these compounds arises from ‘orbital ordering’ brought about by an antiferrodistortive displacement of the halide ions within the basal plane, which is in turn the result of Jahn–Teller distortion of the CuCl_6 octahedra. The latter are elongated (the common sense of distortion in Cu^{II} complexes), but the principal axis of elongation lies within the basal plane and on alternate sites is oriented along [100] and [010] directions of the parent K_2NiF_4 -like unit-cell. As a consequence the single unpaired electron at each Cu^{II} ($3d^9$) site occupies an $(x^2 - y^2)$ orbital, such orbitals being rendered orthogonal to one another by the cooperative Jahn–Teller distortion.

The other electron configuration giving rise to strong Jahn–Teller distorted environments in the d-block elements is d^4 , exemplified by Cr^{II} . It has been found by single crystal neutron diffraction that the $(\text{CrCl}_4)_n^{2n-}$ layers in the prototype salt Rb_2CrCl_4 have an antiferrodistortive order quite similar to that observed in K_2CuF_4 and $(\text{RNH}_3)_2\text{CuCl}_4$ (Day *et al.* 1979; Münnighof *et al.* 1980; Janke *et al.* 1983). Furthermore, polarized neutron diffraction (Münnighof *et al.* 1982) has confirmed orbital ordering, with an electron configuration $(xy)^1(xz)^1(yz)^1(z^2)^1$ on each Cr^{II} , the principal axes of adjacent Cr sites being orthogonal, and the exchange interaction between them ferromagnetic. Since the ground state has $S = 2$, in contrast to $S = \frac{1}{2}$ for d^9 , one anticipates that comparable values of near-neighbour exchange constants will result in higher Curie temperatures. Table 1 collects some data on the unit-cell parameters, near-neighbour exchange constants (J) and Curie temperatures (T_C) for the Cu^{II} (de Jongh & Miedema 1974) and Cr^{II} (Bellitto & Day 1978; Stead & Day 1982) layer perovskite chloride salts containing mono-alkylammonium cations. Values of J are found by

measuring the susceptibility in the paramagnetic temperature range and applying a high-temperature series expansion appropriate to a quadratic layer Heisenberg ferromagnet. Comparing the susceptibilities of $(C_xH_{2x+1}NH_3)_2CrCl_4$ salts with $x = 3, 5, 12$ (figure 5) we see that J is not affected by further separation of the $(CrCl_4)_n^{2n-}$ layers.

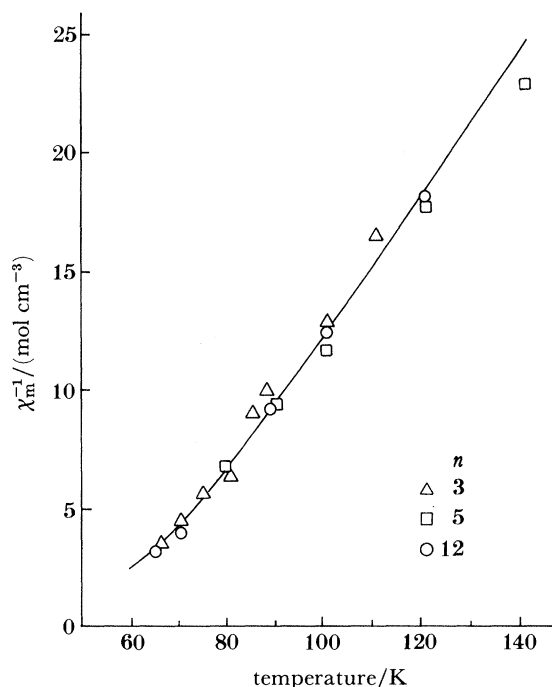


FIGURE 5. Inverse molar susceptibility of $(C_nH_{2n+1}NH_3)_2CrCl_4$ ($B = 1.26$ T). The points are taken from Stead & Day (1982). The line is calculated from the high-temperature series expansion of Rushbrooke & Wood (1958), modified by Lines (1970) for a quadratic layer Heisenberg ferromagnet.

TABLE 1. STRUCTURAL AND MAGNETIC PARAMETERS FOR TWO-DIMENSIONAL HEISENBERG FERROMAGNETS $(C_nH_{2n+1}NH_3)_2MCl_4$ ($M = Cu, S = \frac{1}{2}$; $M = Cr, S = 2$)

n		1	2	3	5	12
Cr	a_0	7.43 ^a	7.79 ^a	7.61 ^b	7.47 ^b	7.45 ^b
	b_0	7.27	7.36	7.36	7.37	7.20
	c_0	18.89	21.41	24.71	35.26	62.1
	J/k_B	6.45 ^a	5.1 ^a	4.6 ^b	4.6 ^b	4.6 ^b
	T_C/K	40.25 ^c	40.60 ^c	—	—	—
Cu	a_0	7.54 ^d	7.47 ^d	7.65 ^d	7.51 ^d	—
	b_0	7.30	7.35	7.33	7.38	—
	c_0	18.55	21.18	24.66	34.81	—
	J/k_B	19.2 ^c	18.6 ^c	16.0 ^c	15.9 ^c	—
	T_C/K	8.91 ^e	10.20 ^e	7.65 ^c	7.30 ^c	—

(a) Bellitto & Day (1978); (b) Stead & Day (1982); (c) A. K. Gregson and N. Moxon quoted in Bellitto *et al.* (1981); (d) de Jongh *et al.* (1969); (e) de Jongh & Miedema (1974).

In addition to a higher T_C two other important consequences follow from the fact that $S > \frac{1}{2}$ in the ground states of the Cr^{II} salts. First is the existence of single-ion anisotropy, which opens a gap in the magnon density-of-states at the Brillouin zone centre. Such anisotropy is required

by theory to achieve a transition to a long-range ordered state at finite temperature (Mermin & Wagner 1966). There has been much discussion about the mechanism of the phase transition to long-range order in a purely two-dimensional magnetic lattice (Lines 1967, 1971; Salamon & Ikeda 1973), including the preparation of literally two-dimensional arrays of Mn^{II} ions by incorporating them into monolayers by the Langmuir–Blodgett technique (Pomerantz *et al.* 1978). In the present case the observed T_{C} s are, as expected, far below those predicted by mean field theory (103 and 81 K for the CH_3NH_3^+ and $\text{CH}_3\text{CH}_2\text{NH}_3^+$ salts respectively), but quite close to the predictions of Stanley–Kaplan (1966) theory for a purely two-dimensional transition (43 and 33 K for the same two salts).

The second consequence of having $S > \frac{1}{2}$ is the appearance of spin-forbidden ligand-field transitions in the optical absorption spectrum. Indeed, such transitions (of quintet-to-triplet type) constitute the only visible absorption in the Cr^{II} salts, since the spin-allowed ligand-field transitions are in the near infrared and charge transfer absorption in the ultraviolet (Bellitto & Day 1976). In magnetically ordered lattices spin-forbidden transitions can acquire electric-dipole strength by associating the creation of a Frenkel exciton to absorption or emission of a magnon with equal and opposite wavevector (Shinagawa & Tanabe 1971). If the exciton has a lower spin projection than the ground state, its formation must be compensated by a positive spin deviation elsewhere in the lattice. This is easy to achieve in an antiferromagnet by creating a magnon on the other sublattice. In a fully magnetized ferromagnet, however, no such possibility exists, but at finite temperature electric-dipole intensity is gained by combining exciton creation with annihilation of thermally populated magnons. The oscillator strength of the visible absorption in the ferromagnetic Cr^{II} salts is therefore strikingly temperature dependent, since it varies as the Bose population factor of the magnons (Day *et al.* 1973). In a two-dimensional square planar Heisenberg ferromagnet the latter takes a very simple form, and at temperatures high compared to the thermal energy of the anisotropy gap (about 1–2 K, see below) but low compared to T_{C} the oscillator strength is predicted (Gregson *et al.* 1976) to vary as T^2 , (figure 6). In all, from room temperature to 4 K the oscillator strength decreases more than two orders of magnitude, producing a colour change seen quite easily with the naked eye.

Further interest attaches to the variation of these absorption band profiles with temperature at the extremes of low and high temperature. In the prototype salt Rb_2CrCl_4 single ion anisotropy produces a gap in the magnon density-of-states at the Brillouin zone centre estimated as 0.808 cm^{-1} from inelastic scattering of long-wavelength neutrons (Hutchings *et al.* 1981). As the temperature is lowered towards 1 K the intensities of the magnon-annihilation sidebands in the optical absorption spectrum begin to depart from the T^2 law as thermally populated magnons are progressively depopulated (Day *et al.* 1979). Quantitative measurements down to 0.8 K (Janke *et al.* 1982) showed that the intensity of the 630 nm band in Rb_2CrCl_4 varied as $T^2 \exp(-E(0)/k_{\text{B}} T)$, where $E(0)$, the zone-centre gap, was defined as 0.837 cm^{-1} , in good agreement with the value found by inelastic neutron scattering. No inelastic neutron scattering measurements have been made on the $(\text{RNH}_3)_2\text{CrCl}_4$ salts because of the difficulty of growing large enough single crystals of these highly air-unstable compounds. However, the low-temperature absorption spectra can be used to estimate the anisotropy gap and measurements of $(\text{CH}_3\text{NH}_3)_2\text{CrCl}_4$ down to 1.5 K yield an estimate of $E(0) = 1.32 \text{ cm}^{-1}$ (Bellitto *et al.* 1985) (figure 7). This figure is larger than that found for the Rb salt, at least partly because the $(\text{CrCl}_4)_n^{2n-}$ framework is not planar in the salt with the organic cation. This arises from the

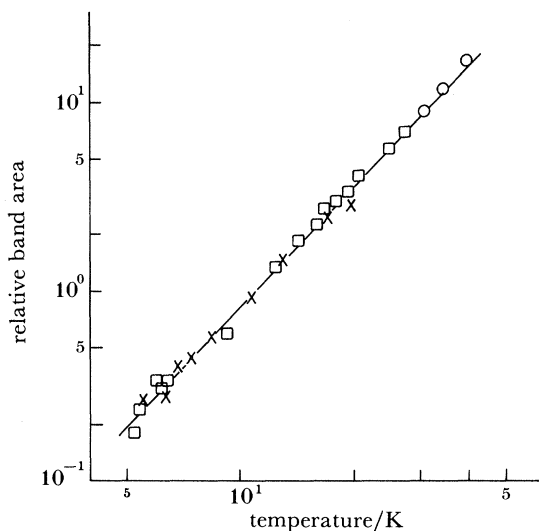


FIGURE 6. Temperature variation of the area of the 540 nm absorption band in $(\text{C}_2\text{H}_5\text{NH}_3)_2\text{CrCl}_4$ (Bellitto & Day 1978).

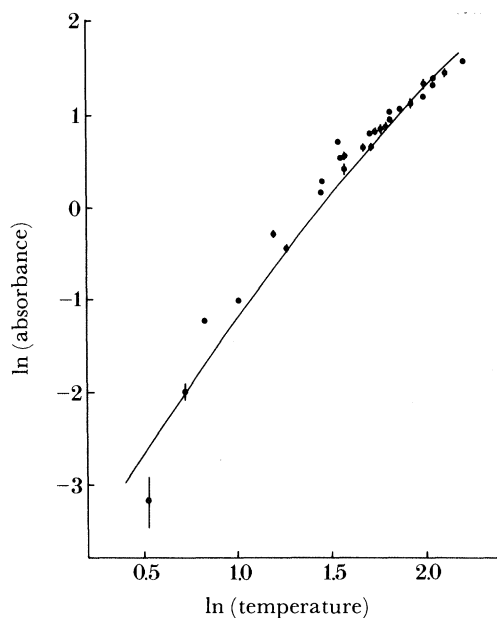


FIGURE 7. Temperature dependence of the area of the 626.8 nm absorption band in $(\text{CH}_3\text{NH}_3)_2\text{CrCl}_4$ below 10 K.

need to accommodate the H-bonding network, and is a feature of all $(\text{RNH}_3)_2\text{MX}_4$. A further consequence of puckering in the inorganic layer is that the principal axes of the local g -tensors at the Cr^{II} sites no longer coincide. Thus there is a small degree of spin canting or, put another way, a small ferromagnetic component in the spin structure. As a result, when most of the intensity of the magnon-annihilation sideband (band (a) in figure 8) has disappeared at low temperature a weak magnon creation sideband (band (b)) becomes apparent.

While the description of the electronic excitations in these salts as Frenkel excitons remains

valid at any temperature, magnons remain well defined only when their wavelength is much shorter than the spin correlation length. The behaviour of the optical absorption band profiles should therefore yield information about the evolution of spin correlation above the three-dimensional ordering temperature, when, in such a strongly two-dimensional lattice, long-range correlations may persist within the layers in the absence of any correlation between them. It is notable that the intensities of the visible absorption bands begin to fall sharply at temperatures well above T_C . If the intensity I is plotted in the reduced form $[I(\infty) - I(T)]/I(\infty)$ against temperature T it is clear that no sharp break occurs in the plot at T_C (figure 9), when the infinite range correlation function Γ_∞ drops sharply to zero (Bellitto *et al.* 1980). There have been numerous treatments of spin correlations in two-dimensional Heisenberg magnets since the original proof by Mermin & Wagner (1966) that no long range order should exist above 0 K. Most pertinent to the results of figure 9 is the approach of Villain (1974) who used a 'semi-polar'

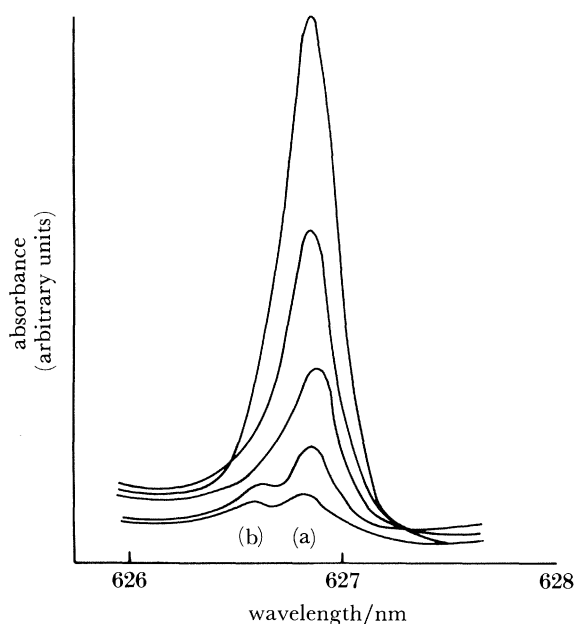


FIGURE 8. Absorption spectra of $(\text{CH}_3\text{NH}_3)_2\text{CrCl}_4$ in the 627 nm region. From top to bottom the spectra were recorded at 4.21, 3.26, 2.68, 2.03, 1.69 K. (a) is the magnon annihilation sideband and (b) the magnon creation sideband.

representation to define magnons of any wavelength in a one- or two-dimensional lattice, even when there is no long-range order, provided there is an easy plane (as indeed exists in the present case). In this theory the static correlation function Γ_r at short distance r in a two-dimensional magnet is a Gaussian function of r , with exponent proportional to T^3/DJ^2 , where D is the planar anisotropy constant and J the near-neighbour exchange constant. The temperature dependence of Γ_1 from Villain's theory is plotted in figure 9 for parameter values appropriate to $(\text{RNH}_3)_2\text{CrCl}_4$. Agreement with the intensity data for CH_3NH_3^+ , $\text{C}_2\text{H}_5\text{NH}_3^+$ and $\text{C}_8\text{H}_{17}\text{NH}_3^+$ salts is quite satisfactory, and clearly demonstrates the importance of short-range correlations in these two-dimensional ferromagnets.

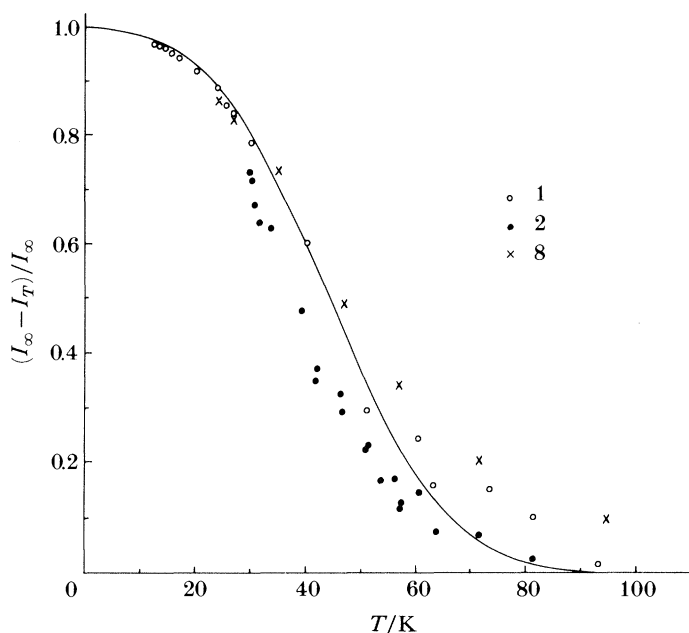
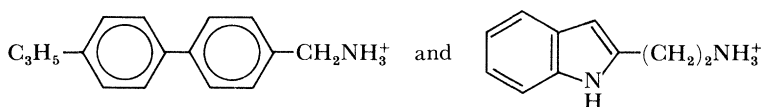


FIGURE 9. Area of the 530 nm band $I(T)$ in $(C_nH_{2n+1}NH_3)_2CrCl_4$ as a function of temperature. The line is I_1 calculated from the theory of Villain (1974) for $J = 9.0 \text{ cm}^{-1}$ and anisotropy $D = 0.3 \text{ cm}^{-1}$.

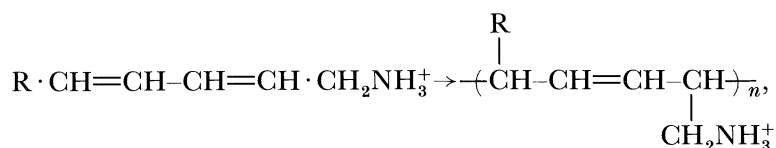
5. POLYMERIZATION OF ORGANIC MOEITIES BETWEEN INORGANIC LAYERS

So far we have only considered n -alkyl chains as the organic moieties in organic-inorganic composite compounds. These pack with their chains parallel and pointing away from the inorganic layer. Within the steric constraints imposed by the stoichiometry of the composite compound, which sets a limit on the 'density' at which organic groups can be packed together over a given area of the inorganic layer, it should be possible to accommodate a wide variety of different groups. Then stereospecific interactions need to be considered and, in particular, polymerizations might be engineered following the 'topochemical principle'. The latter states that reactions between molecules in crystals take place with greatest facility when there is the smallest possible displacement of individual atoms or molecules from the initial crystal to the product (Cohen & Schmidt 1964). The most striking example of the topochemical principle so far encountered among solid state polymerizations is that of the various derivatives of hexane-2,4-diyne, commonly called polydiacetylenes (Wegner 1977). The chemistry and physics of these highly ordered conjugated polymer crystals is reviewed in the contribution of Professor Bloor to this Discussion Meeting.

First attempts to insert more elaborate groups than n -alkyl chains into layer perovskite halide salts centred on conjugated aromatics and on aliphatic chains containing isolated $-C=C-$ or $-C\equiv C-$ bonds. Cations related to the p'' -substituted-4'-cyano-4'-biphenyls, which are well known for their mesomorphic behaviour, and ones related to aromatic heterocycles like indole can be inserted:



have been prepared in our laboratory as tetrachloromanganate(II) salts, for example. The latter has optical spectra characteristic of two-dimensional antiferromagnetic behaviour (Haber 1980). Compounds such as $(\text{CH}\equiv\text{C}\cdot\text{CH}_2\text{NH}_3)_2\text{CdCl}_4$ and $(\text{CH}_2=\text{CH}\cdot\text{CH}_2\text{NH}_3)_2\text{CdCl}_4$ remain stable to irradiation from a high pressure H_2 lamp (Ledsham & Day 1981), as do compounds containing a $-\text{C}=\text{C}-$ bond in the centre of an n -alkyl chain such as $(\text{CH}_3(\text{CH}_2)_7\text{CH}=\text{CH}(\text{CH}_2)_8\text{NH}_3)\text{CdCl}_4$. However, there are two cases where polymerization within layer perovskite halide lattices has been demonstrated. Tieke & Wegner (1981) reported that salts of 6-amino-hexane-2,4-dienoic acid polymerize on irradiation at 254 nm to form 1,4-disubstituted-*trans*-polybutadienes:



This is an unusual reaction because 1,4-addition polymerization of 1,4-disubstituted-*trans*, *trans*-dienes had not been observed previously in the solid. The product is not conjugated, so no enhanced conductivity is to be expected, but the existence of a reaction of this kind may point the way towards reaction that could yield such a polymer.

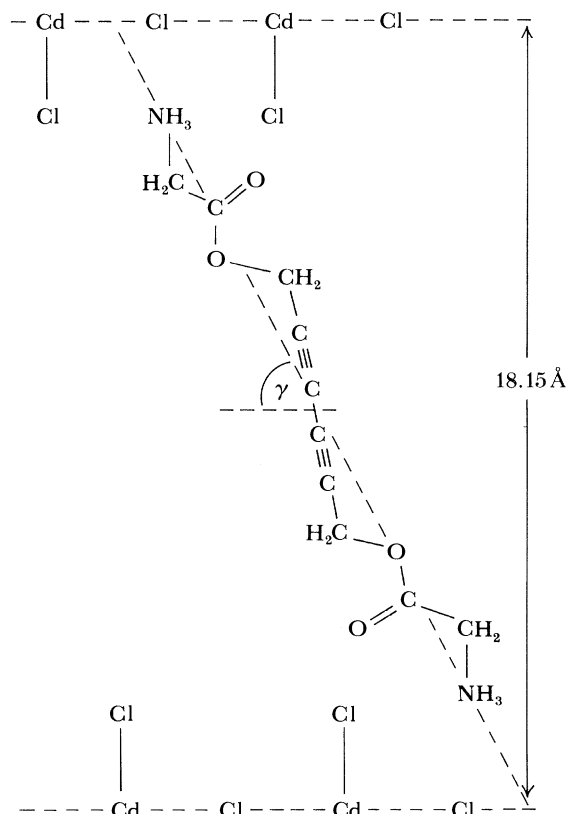
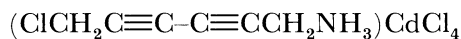
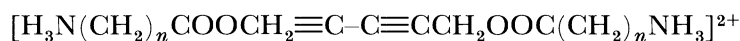


FIGURE 10. Estimated conformation of a diacetylenic layer perovskite halide salt.

Given the high degree of order in the polydiacetylene polymers it appeared worthwhile to attempt polymerization of quaternary ammonium cations based on the substituted hexane-2,4-diyne backbone, in the form of layer perovskite halide salts (Ledsham & Day 1981; Day & Ledsham 1982). A direct approach is to chlorinate the photochemically stable hexane-2,4-diyne-1,6-diol with SOCl_2 in pyridine and convert the 1,6-dichloro-compound to the 1-chloro-6-amino-compound with hexamethylenetetramine in CHCl_3 . The salt



polymerizes very rapidly, but does not remain monocrystalline. An alternative, and more flexible, approach to amino-substituted diacetylenic monomers is to esterify the 1,6-diol with an ω -amino carboxylic acid, protecting the amino-group with di-tert-butyl carbonate. The tetrachlorocadmium salt of the di-cation



polymerizes very rapidly for $n = 5$ but only slowly for $n = 1$, so that unit-cell parameters can be obtained for the monomer salt. By using known bond lengths and angles from related compounds the conformation shown in figure 10 can be estimated. The most important factors in the efficient solid-state polymerization of the diacetylenes are the distance d between the centres of neighbouring $-\text{C}\equiv\text{C}-\text{C}\equiv\text{C}-$ units, which should lie between 4.5 and 5.7 Å and the angle γ between the axis of the unit and the line joining neighbouring units, which should be in the region of 45°. The conformation shown in figure 10 permits a d of 5.2 Å but γ is 70–80°, which is probably why the polymerization only proceeds slowly.

6. CONCLUSION: MOLECULAR ENGINEERING IN THE SOLID STATE

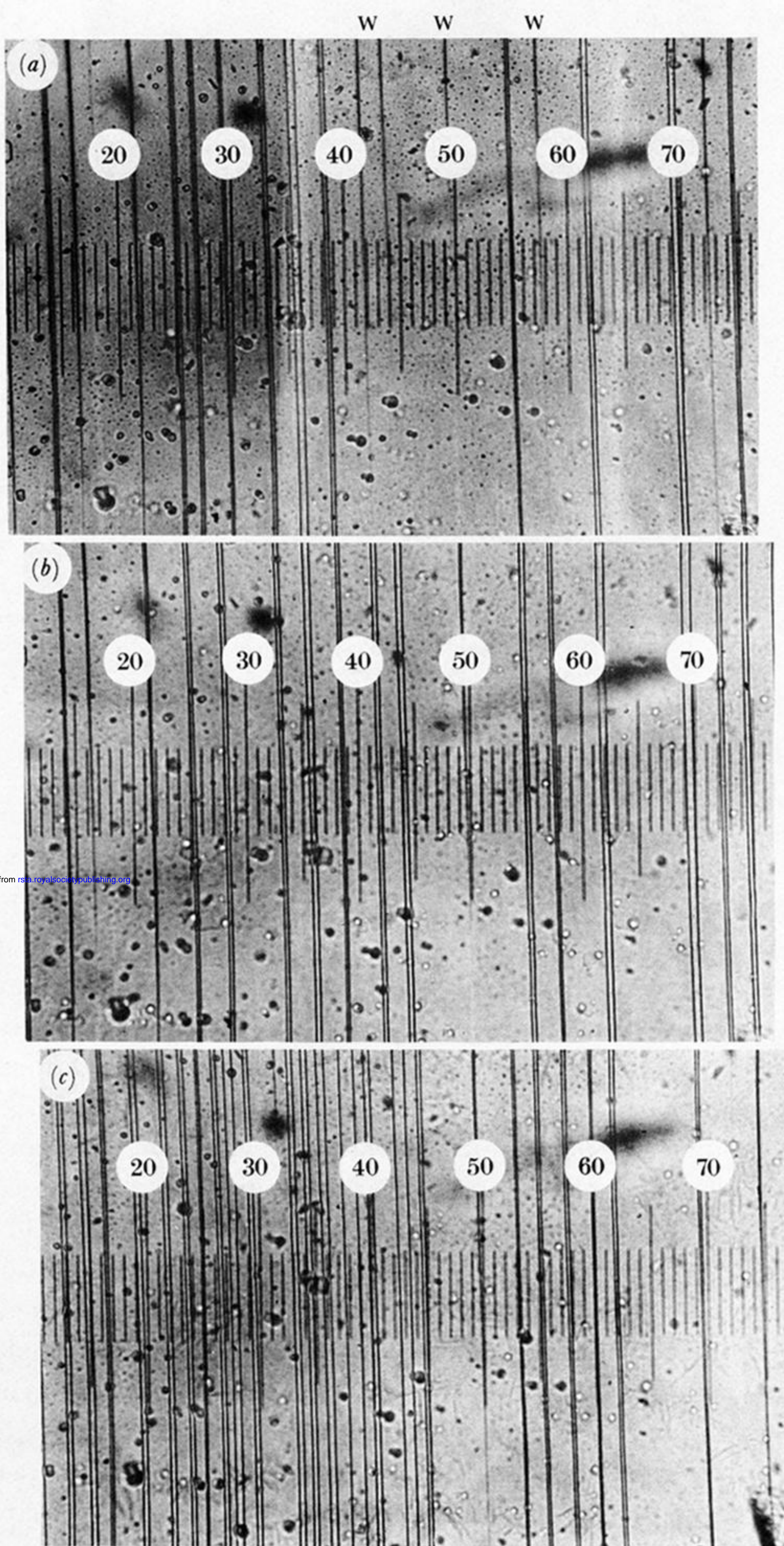
In this contribution I have summarized work on phase transitions, electronic properties and chemical reactions in one particular class of organic-inorganic layer 'molecular composites'. Such lattices have great chemical flexibility, leading to a wide range of interesting and unusual phenomena. Chemical synthesis will undoubtedly reveal more: the nature of the inorganic layer can be changed, together with the means of attaching organic groups, as well as the organic groups themselves. For example, no work has been reported yet on incorporation of molecules like tetrathio- or tetraselenofulvalenes, which form the basis of molecular metals and superconductors. Conducting inorganic layers with covalently bonded organic sidechains have not yet been synthesized. Melting of sidechains might be exploited to enable molecular composites to function as two-dimensional solvents for incoming molecules. In summary, opportunities for molecular and crystal engineering in layer composites are quite extensive.

The experiments summarized here have been made by numerous postdoctoral, graduate and fourth year undergraduate students, whose names appear in the references. Our group has been generously funded by S.E.R.C.

REFERENCES

- Arend, H. & Granicher, H. 1976 *Ferroelectrics* **13**, 537.
 Arend, H., Hofmann, R. & Waldner, F. 1973 *Solid St. Commun.* **13**, 1629.
 Arend, H., Huber, W., Mischgofsky, F. H. & Richter-van Leeuwen, G. K. 1978 *J. Cryst. Growth* **42**, 213.

- Avery, N. W. J. 1984 Chemistry part II thesis, University of Oxford.
- Bellitto, C. & Day, P. 1976 *J. chem. Soc. chem. Commun.*, pp. 870.
- Bellitto, C. & Day, P. 1978 *J. chem. Soc. Dalton Trans.*, pp. 1207.
- Bellitto, C., Fair, M. J., Wood, T. E. & Day, P. 1980 *J. Phys. C* **13**, L627.
- Bellitto, C., Wood, T. E. & Day, P. 1985 *Inorg. Chem.* (In the press.)
- Blinic, R., Burger, M., Lozar, B., Seliger, J., Slak, J., Rutar, V., Arend, H. & Kind, R. 1977 *J. chem. Phys.* **66**, 278.
- Cohen, M. D. & Schmidt, G. M. J. 1964 *J. chem. Soc.*, pp. 1996.
- Day, P., Gregson, A. K. & Leech, D. H. 1973 *Phys. Rev. Lett.* **30**, 19.
- Day, P., Hutchings, M. J., Janke, E. & Walker, P. J. 1979 *J. chem. Soc. chem. Commun.*, pp. 711.
- Day, P., Janke, E., Wood, T. E. & Woodwark, D. 1979 *J. Phys. C* **12**, L329.
- Day, P. & Ledsham, R. D. 1982 *Molec. Cryst. liq. Cryst.* **86**, 163.
- de Jongh, L. J. & Miedema, A. R. 1974 *Adv. Phys.* **24**, 1.
- Gregson, A. K., Day, P., Okiji, A. & Elliott, R. J. 1976 *J. Phys. C* **9**, 4497.
- Haber, V. 1980 In *Proc. 8th Conf. on Coord. Chem., Smolenice, Czech.*, p. 111.
- Heger, G., Mullen, D. & Knorr, K. 1976 *Physica. Status. Solidi. A* **35**, 627.
- Heygstar, G. & Kleeman, W. 1977 *Physica* **89B**, 165.
- Hutchings, M. T., Als-Neilsen, J., Lindgard, P. A. & Walker, P. J. 1981 *J. Phys. C* **14**, 5327.
- Janke, E., Hutchings, M. T., Day, P. & Walker, P. J. 1983 *J. Phys. C* **16**, 5989.
- Janke, E., Wood, T. E., Ironside, C. & Day, P. 1982 *J. Phys. C* **15**, 3809.
- Kind, R., Plesko, S., Arend, H., Blinic, R., Zeks, B., Seliger, J., Lozar, B., Slak, J., Levstik, A., Felipic, C., Zagar, V., Lahajnar, G., Milia, F. & Chapius, G. 1979 *J. chem. Phys.* **71**, 2118.
- Ledsham, R. D. & Day, P. 1981 *J. chem. Soc. chem. Commun.*, pp. 921.
- Lines, M. E. 1970 *J. Phys. Chem. Solids* **31**, 101.
- Lines, M. E. 1971 *Phys. Rev. B* **3**, 1749.
- Little, W. A. 1964 *Phys. Rev. A* **135**, 1416.
- Mathey, Y., Mazieres, C., Gourdjji, M. & Guibe, L. 1980 *Molec. Phys.* **37**, 693.
- Mermin, N. D. & Wagner, H. 1966 *Phys. Rev. Lett.* **17**, 1133.
- Mostafa, M. F. & Willett, R. D. 1971 *Phys. Rev. B* **4**, 2213.
- Münninghof, G., Hellner, E., Fyne, P. J., Day, P., Hutchings, M. T. & Tasset, F. 1982 *J. Phys., Paris C* **7**, **43**, 243.
- Münninghof, G., Treutmann, W., Hellner, E., Heger, G. & Reinen, D. 1980 *J. solid St. Chem.* **34**, 289.
- Pomerantz, M., Dracol, F. H. & Segmuller, A. 1978 *Phys. Rev. Lett.* **40**, 246.
- Rushbrooke, G. S. & Wood, P. J. 1958 *Molec. Phys.* **1**, 257.
- Salamon, M. B. & Ikeda, H. 1973 *Phys. Rev. B* **7**, 2017.
- Shinagawa, K. & Tanabe, Y. 1971 *J. phys. Soc. Japan* **30**, 1280.
- Stanley, H. E. & Kaplan, T. A. 1966 *Phys. Rev. Lett.* **17**, 913.
- Stead, M. J. & Day, P. 1982 *J. chem. Soc. Dalton Trans.*, pp. 1081.
- Tieke, B. & Wegner, G. 1981 *Makromol. Chem., Rapid Commun.* **2**, 543.
- Van Amstel, W. D. & de Jongh, L. J. 1971 *Solid St. Commun.* **11**, 1423.
- Villain, J. 1974 *J. Phys., Paris* **35**, 27.
- Wegner, G. 1977 In *Molecular metals* (ed. W. E. Hatfield). New York: Plenum Press.
- Yamanaka, S., Sakamoto, K. & Hatton, M. 1981 *J. phys. Chem.* **85**, 1930.



Downloaded from rsta.royalsocietypublishing.org

FIGURE 3. Twinning domains in a crystal of $(\text{CH}_3\text{NH}_3)_3\text{MnCl}_4$ after heating through the r.t.o. \rightarrow h.t.t. phase transition, annealing for different times and cooling. Annealing times are (a) 10 min (b) 100 min (c) 900 min.

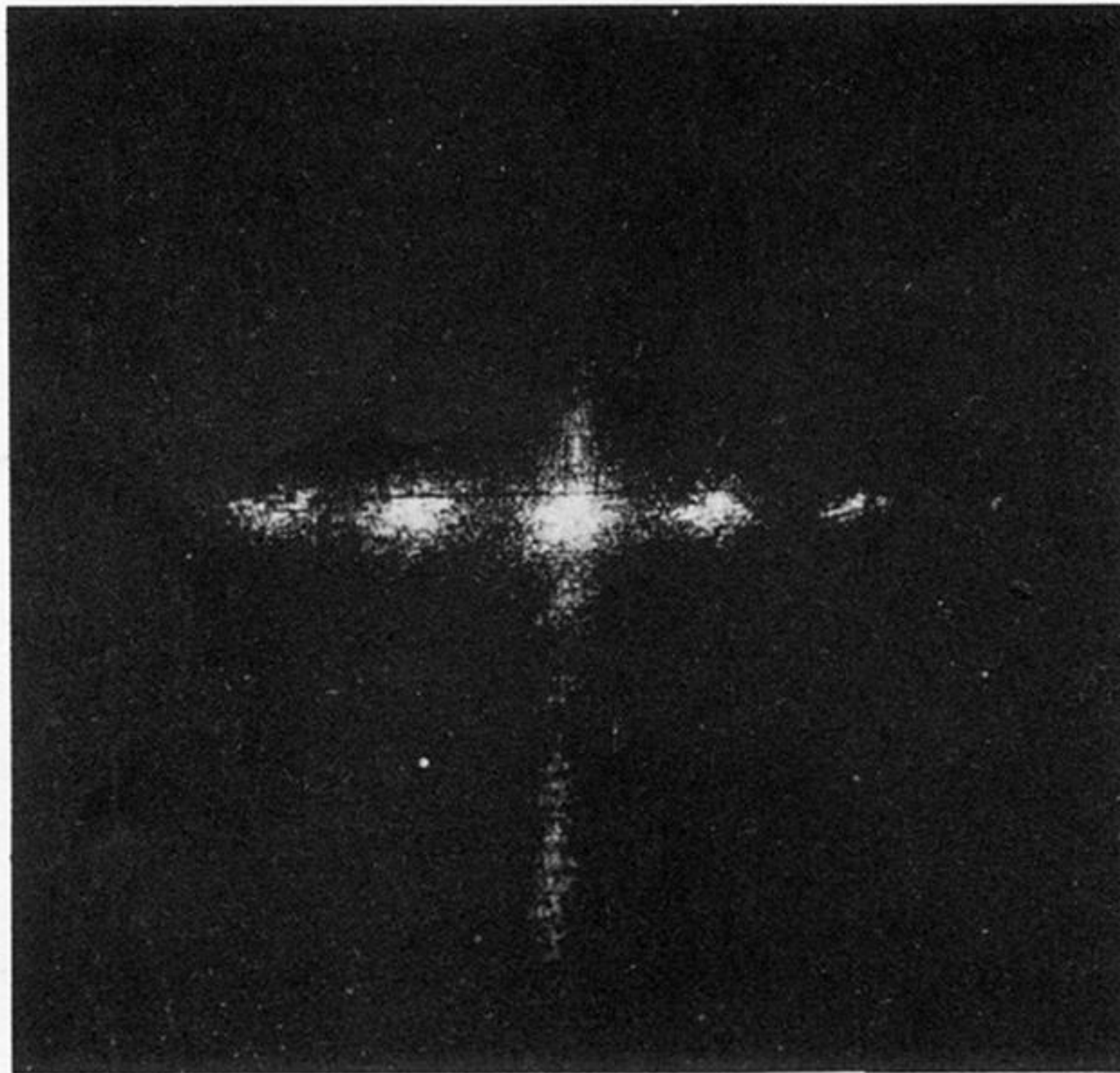


FIGURE 4. Optical diffraction pattern from transmission of 6328 Å light through a crystal of $(\text{CH}_3\text{NH}_3)_2\text{MnCl}_4$ at room temperature.